

MODEL-PREDICTIVE POLICY LEARNING WITH UNCERTAINTY REGULARIZATION FOR DRIVING IN DENSE TRAFFIC

Anonymous authors

Paper under double-blind review

ABSTRACT

Learning a policy using only observational data is challenging because the distribution of states it induces at execution time may differ from the distribution observed during training. In this work, we propose to train a policy while minimizing a measure of the mismatch between these two distributions. We obtain estimates of the distribution induced by the policy using a learned dynamics model, and propose a general, differentiable measure of the distribution mismatch using uncertainty estimates of the dynamics model’s predictions, calculated using dropout. Our framework also naturally yields a model-based imitation learning algorithm when the observational data consists of expert trajectories. We evaluate both approaches using a large-scale observational dataset of driving behavior recorded from traffic cameras, and show that we are able to learn effective driving policies from purely observational data, with no environment interaction.

1 INTRODUCTION

In recent years, model-free reinforcement learning methods using deep neural network controllers have proven effective on a wide range of tasks, from playing video or text-based games (Mnih et al., 2015; 2016; Narasimhan et al., 2015) to learning algorithms (Zaremba et al., 2015) and complex locomotion tasks (Lillicrap et al., 2015; Zhang et al., 2015). However, these methods often require a large number of interactions with the environment in order to learn. While this is not a problem if the environment is simulated, it can limit the application of these methods in realistic environments where interactions with the environment are slow, expensive or potentially dangerous. Building a simulator where the agent can safely try out policies without facing real consequences can mitigate this problem, but requires human engineering effort which increases with the complexity of the environment being modeled.

Model-based reinforcement learning approaches try to learn a model of the environment dynamics, and then use this model to plan actions or train a parameterized policy. A common setting is where an agent alternates between collecting experience by executing actions using its current policy or dynamics model, and then using these experiences to improve its dynamics model. This approach has been shown empirically to significantly reduce the required number of environment interactions (Atkeson & Santamaria, 1997; Deisenroth & Rasmussen, 2011; Nagabandi et al., 2017; Chua et al., 2018).

Despite these improvements in sample complexity, there exist settings where even a *single* poor action executed by an agent in a real environment can have consequences which are not acceptable. At the same time, with data collection becoming increasingly inexpensive, there are many settings where observational data of an environment is abundant. This suggests a need for algorithms which can learn policies primarily from observational data, which can then perform well in a real environment. Autonomous driving is an example of such a setting: on one hand, trajectories of human drivers can be easily collected using traffic cameras (Halkias & Colyar, 2006), resulting in an abundance of observational data; on the other hand, learning through interaction with the real environment is not a viable solution.

However, learning policies from purely observational data is challenging because the data may only cover a small region of the space over which it is defined. If the observational data consists of state-action pairs produced by an expert following an optimal policy, one option is to use imitation learning (Pomerleau, 1991). However, passive imitation learning is well-known to suffer from a mismatch between the states seen at training and execution time (Ross & Bagnell, 2010), and may need to be augmented by querying an expert (Ross et al., 2011). Another option is to learn a dynamics model from observational data, and then use it to train a policy. However, the dynamics model may make arbitrary predictions outside the domain it was trained on, which may wrongly be associated with low cost (or high reward) as shown in Figure 1. The policy network may then exploit these errors in the dynamics model and produce actions which lead to these wrongly optimistic states. In the interactive setting, this problem is naturally self-correcting, since states where the model predictions are wrongly optimistic will be more likely to be experienced, and thus will correct the dynamics model. However, the problem persists if the dataset of environment interactions which the model is trained on is fixed.

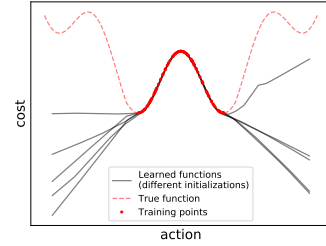


Figure 1: Different models fitted on training points which cover a limited region the function’s domain. Models make arbitrary predictions outside of this region.

In this work, we propose to train a policy while explicitly penalizing the mismatch between the distribution of trajectories it induces and the one reflected in the training data. We do this by using a learned dynamics model which is unrolled for multiple time steps, and training a policy network to minimize a differentiable cost over this rolled-out trajectory. This differentiable cost contains two terms: a policy cost which represents the objective the policy seeks to optimize, and an uncertainty cost which represents its divergence from the states it is trained on. We propose to measure this second cost by using the uncertainty of the dynamics model about its own predictions, calculated using dropout. We evaluate our approach in the context of learning policies to drive an autonomous car in dense traffic, using a large-scale dataset of real-world driving trajectories which we also adapt into an environment for testing learned policies; both dataset and environment will be made public. We show in our experiments that model-based control using this additional uncertainty regularizer substantially outperforms unregularized control, and enables learning good driving policies using only observational data with no environment interaction or additional labeling by an expert.

2 MODEL-PREDICTIVE POLICY LEARNING WITH UNCERTAINTY REGULARIZATION

We assume we are given a dataset of observational data which consists of state-action pairs $\mathcal{D} = \{(s_t, a_t)\}_t$. We first describe our general approach, which consists of two steps: learning an action-conditional dynamics model using the collected observational data, and then using this model to train a fast, feedforward policy network which minimizes both a policy cost and an uncertainty cost.

2.1 ACTION-CONDITIONAL FORWARD MODEL

The dynamics model can be deterministic or stochastic. A deterministic model $f_\theta(s_{1:t}, a_t)$ takes as input a sequence of observed or previously predicted states $s_{1:t}$ and an action a_t , and produces a prediction of the next state \hat{s}_{t+1} . The per-sample loss which it minimizes is given by $\ell(s_{t+1}, \hat{s}_{t+1})$, where ℓ is a loss function appropriate for the task at hand. A stochastic model additionally takes as input a latent variable z_t which represents the information about the next state s_{t+1} which is not a deterministic function of the input. In this work, we consider recent approaches for stochastic prediction based on Variational Autoencoders (Kingma & Welling, 2013; Babaeizadeh et al., 2017; Denton & Fergus, 2018), but other approaches could be used as well. During training, latent variables are sampled from a posterior network $q_\phi(s_{1:t}, s_{t+1})$ which outputs the parameters (μ_ϕ, σ_ϕ) of a diagonal Gaussian distribution conditioned on the past inputs and true targets. This network is trained jointly with the rest of the model using the reparameterization trick, and a term is included in the loss to minimize the KL divergence between the posterior distribution and a fixed prior $p(z)$, which in our case is an isotropic Gaussian. After training, different future predictions for a given sequence of frames can be generated by sampling different latent variables from the prior distribution.

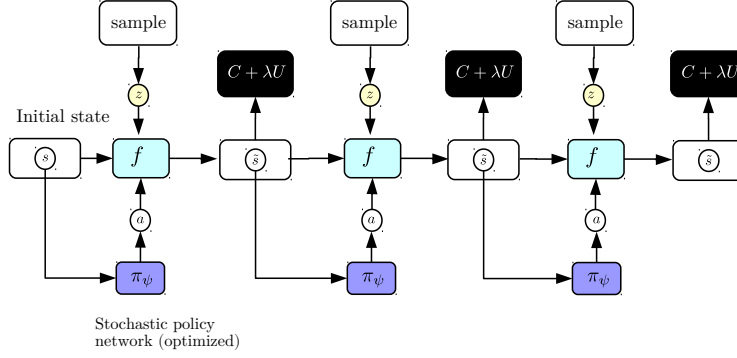


Figure 2: Training the policy network using the stochastic forward model. Gradients with respect to costs associated with predicted states are passed through the unrolled forward model into a policy network.

2.2 TRAINING A POLICY NETWORK WITH UNCERTAINTY MINIMIZATION

Once the forward model is trained, we use it to train a parameterized policy network π_ψ , which we assume to be stochastic. We first sample an initial state sequence $s_{1:t}$ from the training set, unroll the forward model over T time steps, and backpropagate gradients of a differentiable objective function with respect to the parameters of the policy network. During this process the weights of the forward model are fixed, and only the weights of the policy network are optimized. This objective function contains two terms: a *policy cost* C , which reflects the underlying objective the policy is trying to learn, and an *uncertainty cost* U , which reflects how close the predicted state induced by the policy network is to the manifold which the data \mathcal{D} is drawn from. In the case of the deterministic model, training the policy involves solving the following problem:

$$\operatorname{argmin}_{\psi} \left[\sum_{i=1}^T C(\hat{s}_{t+i}) + \lambda U(\hat{s}_{t+1}) \right], \text{ such that: } \begin{cases} \hat{a}_{t+i} \sim \pi_\psi(s_{t+i-1}) \\ \hat{s}_{t+i} = f(\hat{s}_{t+i-1}, \hat{a}_{t+i}) \end{cases}$$

The stochastic forward model additionally takes as input latent variables sampled from the prior at each time step. The problem then becomes:

$$\operatorname{argmin}_{\psi} \left[\sum_{i=1}^T C(\hat{s}_{t+i}) + \lambda U(\hat{s}_{t+1}) \right], \text{ such that: } \begin{cases} z_{t+i} \sim p(z) \\ \hat{a}_{t+i} \sim \pi_\psi(s_{t+i-1}) \\ \hat{s}_{t+i} = f(\hat{s}_{t+i-1}, \hat{a}_{t+i}, z_{t+i}) \end{cases}$$

The uncertainty cost U is applied to states predicted by the forward model, and could reflect any measure of their likelihood under the distribution the training data is drawn from. We propose here a general form based on the uncertainty of the dynamics model, which is calculated using dropout. Intuitively, if the dynamics model is given a state-action pair from the same distribution as \mathcal{D} (which it was trained on), it will have low uncertainty about its prediction. If it is given a state-action pair which is outside this distribution, it will have high uncertainty.

Dropout (Hinton et al., 2012; Srivastava et al., 2014) is a regularization technique which consists of randomly setting hidden units in a neural network to zero with some probability. The work of (Gal & Ghahramani, 2016) showed that a neural network trained with dropout is equivalent to an approximation of a probabilistic deep Gaussian Process model. A key result of this is that estimates of the neural network’s model uncertainty for a given input can be obtained by calculating the covariance of its outputs taken over multiple dropout masks. We note that this uncertainty estimate is the composition of differentiable functions: each of the models induced by applying a different dropout mask is differentiable, as is the covariance operator. Furthermore, we can summarize the covariance matrix by taking its trace (which is equal to the sum of its eigenvalues, or equivalently the

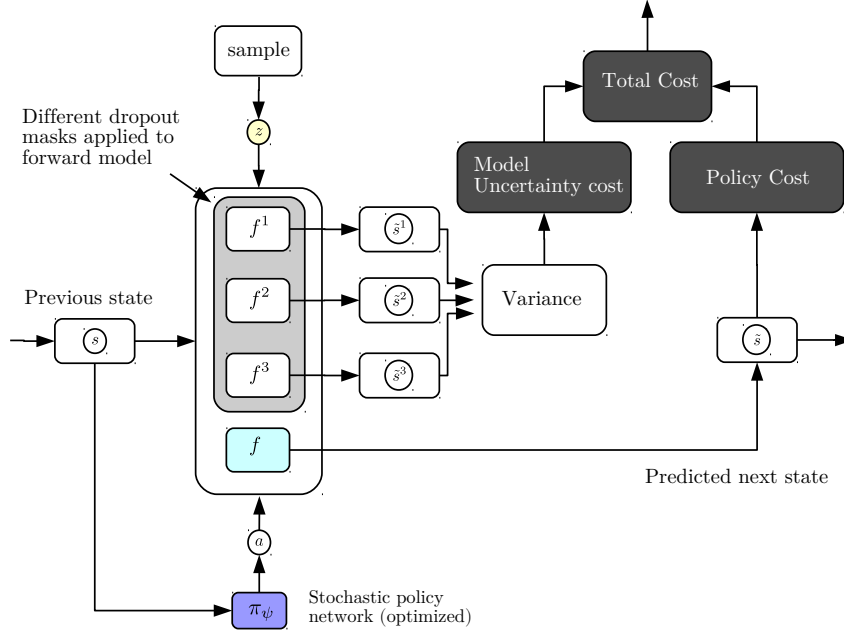


Figure 3: Training the policy network using the differentiable uncertainty cost, calculated using dropout.

sum of the variances of the outputs across each dimension), which is also a differentiable operation. This provides a scalar estimate of uncertainty which is differentiable with respect to the input.

More precisely, let $f_{\theta_1}, \dots, f_{\theta_K}$ denote our prediction model with K different dropout masks applied to its hidden units (this can also be viewed as changing its weights). We define our scalar measure of uncertainty Ω as follows:

$$\begin{aligned}\Omega(s_{1:t}, a_t, z_t) &= \text{tr} \left[\text{Cov}[\{f_{\theta_k}(s_{1:t}, a_t, z_t)\}_{k=1}^K] \right] \\ &= \sum_{j=1}^d \text{Var}(\{f_{\theta_k}(s_{1:t}, a_t, z_t)_j\}_{k=1}^K)\end{aligned}$$

where d is the dimensionality of the output. Minimizing this quantity with respect to actions encourages the policy network to produce actions which, when plugged into the forward model, will produce predictions which the forward model is confident about. To compensate for differences in baseline uncertainty across different modalities or rollout lengths, we estimate the empirical mean and variance of Ω for every rollout length t of the forward model over the training set, to obtain μ_{Ω}^t and σ_{Ω}^t . We then define our uncertainty cost as follows:

$$U(\hat{s}_{t+1}) = U(s_{1:t}, a_t, z_t) = \left[\frac{\Omega(s_{1:t}, a_t, z_t) - \mu_{\Omega}^t}{\sigma_{\Omega}^t} \right]_+ \quad (1)$$

If the uncertainty estimate is lower than the mean uncertainty estimate on the training set for this rollout length, this loss will be zero. These are cases where the model prediction is within normal uncertainty ranges. If the uncertainty estimate is higher, this loss exerts a pull to change the action so that the future state will be predicted with higher confidence by the forward model.

A simple way to define U given an initial sequence of states $s_{1:t}$ from \mathcal{D} would be to set $U(\hat{s}_{t+k}) = \|\hat{s}_{t+k} - s_{t+k}\|$. This would encourage the policy network to output actions which lead to a similar trajectory as the one observed in the dataset. Although this leads to a set of states

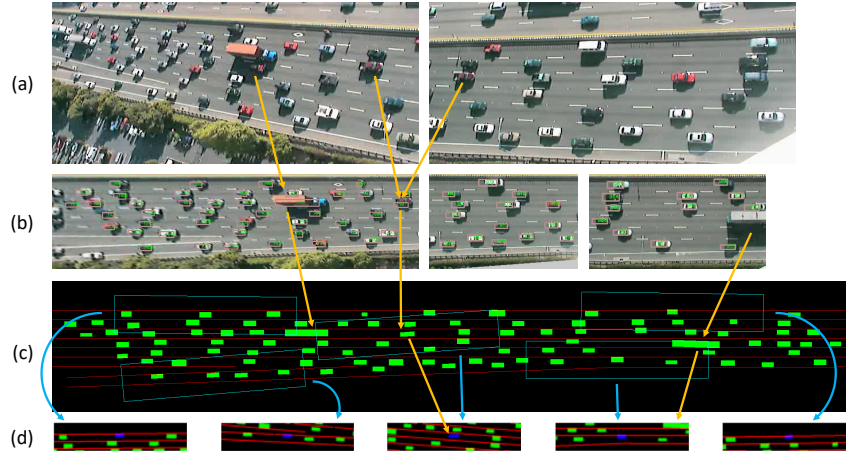


Figure 4: Preprocessing pipeline for the NGSIM-I80 data set. Orange arrows show same vehicles across stages. Blue arrows show corresponding extracted context state. (a) Snapshots from two of the seven cameras. (b) View point transformation, car localisation and tracking. (c) Context states are extracted from rectangular regions surrounding each vehicle. (d) Five examples of context states i_t extracted at the previous stage.

the model is presumably confident about, it may not be a trajectory which also satisfies the policy cost C . The advantage of using the more general cost above is that, assuming the dynamics model generalizes well within its training distribution, there will be multiple trajectories which it will be confident about, and the policy network can then choose one which best satisfies the cost it is trying to optimize. However, if the dataset \mathcal{D} consists of *expert* trajectories, a natural choice would be to set $C(\hat{s}_{t+i}) = U(\hat{s}_{t+i}) = \frac{1}{2} \|\hat{s}_{t+k} - s_{t+k}\|$. This give a model-based imitation learning objective which simultaneously optimizes the policy cost and the uncertainty cost.

3 DATASET AND PLANNING ENVIRONMENT

We apply our approach to learn driving policies using a large-scale dataset of driving videos taken from traffic cameras. The Next Generation Simulation program’s Interstate 80 (NGSIM I-80) dataset (Halkias & Colyar, 2006) consists of 45 minutes of recordings from traffic cameras mounted over a stretch of highway. The driver behavior is complex and includes sudden accelerations, lane changes and merges which are difficult to predict; as such the dataset has high environment stochasticity. After recording, a viewpoint transformation is applied to rectify the perspective, and vehicles are identified and tracked throughout the video. This yields a total 5596 car trajectories, which we split into training (80%), validation (10%) and testing sets (10%).

We then applied additional preprocessing to obtain a state and action representations (s_t, a_t) for each car, suitable for learning an action-conditional predictive model. Our state representation s_t consists of two components: an image i_t representing the neighborhood of the car, and a vector u_t representing its current position and velocity. The images i_t are centered around the ego car and encode both the lane emplacements and the locations of other cars. Each image has 3 channels: the first (red) encodes the lane markings, the second (green) encodes the locations of neighboring cars, which are represented as rectangles reflecting the dimensions of each car, and the third channel (blue) represents the ego car, also scaled to the correct dimensions. This is summarized in Figure 4. We also define two cost functions which together make up the policy cost: a proximity cost which reflects how close the ego car is to neighboring cars, and a lane cost which reflects how much the ego car overlaps with lane markings. These are represented as a cost vector at each timestep, $c_t = (C_{proximity}(s_t), C_{lane}(s_t))$. Full details can be found in Appendix A.

We also adapted this dataset to be used as an environment to evaluate learned policies, with the same interface as OpenAI Gym (Brockman et al., 2016). Choosing a policy for neighboring cars is challenging due to a cold-start problem: to accurately evaluate a learned policy, the other cars would need to follow human-like policies which would realistically react to the controlled car, which are

not available. We take the approach of letting all the other cars in the environment follow their trajectories from the dataset, while a single car is controlled by the policy we seek to evaluate. This approach avoids hand-designing a policy for the neighboring cars which would likely not reflect the diverse nature of human driving. The limitation is that the neighboring cars do not react to the controlled car, which likely makes the problem more difficult as they do not try to avoid collisions.

4 RELATED WORK

A number of authors have explored the use of learned, action-conditional forward models which are then used for planning, starting with classic works in the 90’s (Nguyen & Widrow, 1990; Schmidhuber, 1990; Jordan & Rumelhart, 1992), and more recently in the context of video games (Oh et al., 2015; Pascanu et al., 2017; Weber et al., 2017), robotics and continuous control (Finn et al., 2016; Agrawal et al., 2016; Nagabandi et al., 2017; Srinivas et al., 2018). Our approach to learning policies by backpropagating through a learned forward model is related to the early work of (Nguyen & Widrow, 1989) in the deterministic case, and the SVG framework of (Heess et al., 2015) in the stochastic case. However, neither of these approaches incorporates a term penalizing the uncertainty of the forward model when training the policy network.

The works of (McAllister & Rasmussen, 2016; Chua et al., 2018) also used model uncertainty estimates calculated using dropout in the context of model-based reinforcement learning, but used them for sampling trajectories during the forward prediction step. Namely, they applied different dropout masks to simulate different state trajectories which were then averaged to produce a cost estimate used to select an action.

Our model uncertainty penalty is related to the cost used in (Kahn et al., 2017), who used dropout and model ensembling to compute uncertainty estimates for a binary action-conditional collision detector for a flying drone. These estimates were then used to select actions out of a predefined set which yielded a good tradeoff between speed, predicted chance of collision and uncertainty about the prediction. In our work, we apply uncertainty estimates to the predicted high-dimensional states of a forward model at every time step, summarize them into a scalar, and backpropagate gradients through the unrolled forward model to then train a policy network by gradient descent.

The problem of covariate shift when executing a policy learned from observational data has been well-recognized in imitation learning. It was first noted in the early work of (Pomerleau, 1991), and was shown in (Ross & Bagnell, 2010) to cause a regret bound which grows quadratically in the time horizon of the task. The work of (Ross et al., 2011) proposed a method to efficiently use expert feedback if available, which has also been applied in the context of autonomous driving (Zhang & Cho, 2016). Our approach also addresses covariate shift, but does so without querying an expert.

Our model-based imitation learning algorithm is related to the work of (Englert et al., 2013), who also performed imitation learning at the level of trajectories rather than individual actions. They did so in low-dimensional settings using Gaussian Processes, whereas our method uses an unrolled neural network representing the environment dynamics which can be applied to high-dimensional state representations. The work of (Baram et al., 2017) also used a dynamics model in the context of imitation learning, but did so in the interactive setting to minimize a loss produced by a discriminator network.

Several works have applied deep learning methods in the context of autonomous driving. The works of (Pomerleau, 1991; LeCun et al., 2006; Bojarski et al., 2016; Pan et al., 2017) used neural networks to control policies trained by imitation learning, while (Williams et al., 2017) learned models of the vehicle dynamics. These works focused on lane following or offroad driving in visually rich environments and did not consider settings with dense traffic, which we focus on in this work. The work of (Sadigh et al., 2016) developed a model of the interactions between the two drivers which was then used to plan actions in simple settings, using symbolic state representations. In our work, we consider the problem of learning driving policies in dense traffic, using high-dimensional state representations which reflect the neighborhood of the ego car.

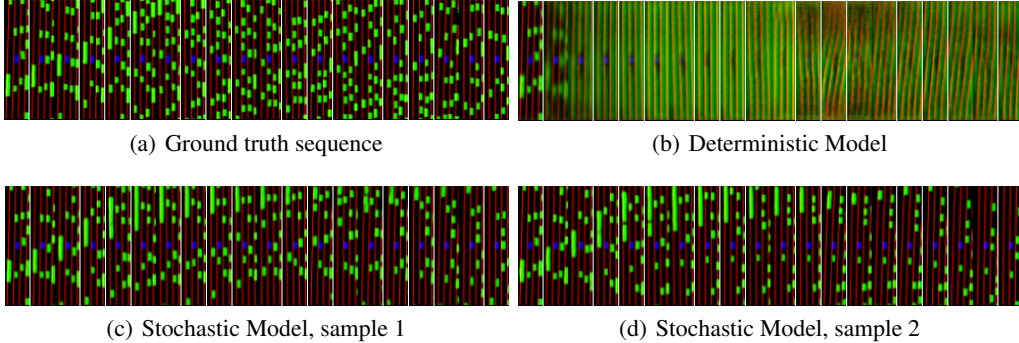


Figure 5: Video prediction results using a deterministic and stochastic model. Two different future predictions are generated by the stochastic model by sampling two different sequences of latent variables. The deterministic model averages over possible futures, producing blurred predictions.

5 EXPERIMENTS

We now report experimental results. We designed a deterministic and stochastic forward model to model the state and action representations described in Section 3, using convolutional layers to process the images i_t and fully-connected layers to process the vectors u_t and actions a_t . All model details can be found in Appendix B and training details can be found in Appendix D.

5.1 PREDICTION RESULTS

We first generated predictions using both deterministic and stochastic forward models, shown in Figure 5. The deterministic model produces predictions which become increasingly blurry further into the future. Our stochastic model produces predictions which stay sharp far into the future. By sampling different sequences of latent variables, different future scenarios are generated. Note that the two sequences generated by the stochastic model are different from the ground truth future which occurs in the dataset. This is normal as the future observed in the dataset is only one of many possible ones. Additional video generations can be viewed at the following URL: <https://youtu.be/wRrQEVLq3dA>.

5.2 POLICY EVALUATION RESULTS

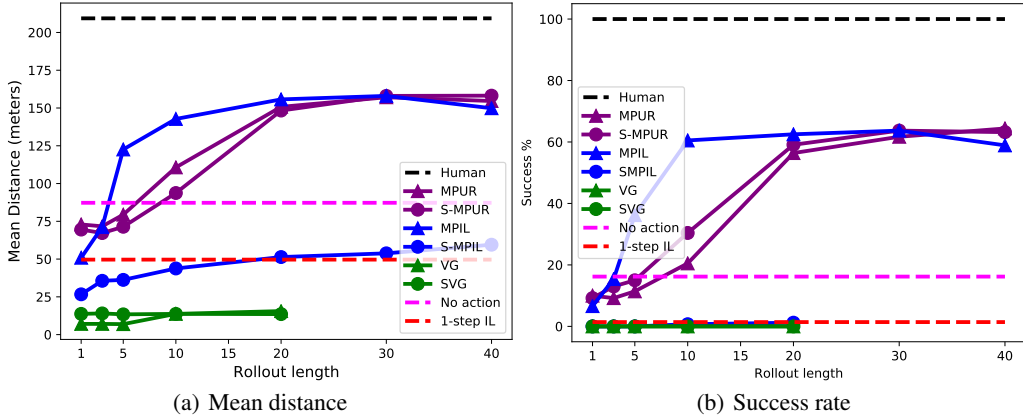
We evaluated different policies using two measures: whether the controlled car reaches the end of the road segment without colliding into another car or driving off the road, and the distance travelled before the episode ends. Policies which collide quickly will travel shorter distances. All cars are initialized at the beginning of the road segment with the initial speed they were driving at in the dataset, and then are controlled by the policy being measured. We only report performance for cars in the testing trajectories, which were not used when training the forward model or policy network.

We compared our approach against several baselines which can also learn from observational data, which are described in Table 5.2c. Full details are contained in Appendix C. All policy networks have the same architecture, and all are fed the concatenation of the 20 previous states as input. They all output the parameters of a 2D diagonal Gaussian over action space, from which the next action is sampled.

The policy cost which we minimize for VG, SVG and MPUR is given by:

$$C = C_{proximity} + 0.2 \cdot C_{lane} \quad (2)$$

where $C_{proximity}$ and C_{lane} are the proximity and lane costs described in Section 3. This puts a higher priority on avoiding other cars while still encouraging the policy to stay within the lanes. MPUR additionally minimizes U , the model uncertainty cost described in Section 2.2. We set $\lambda = 0.01$ for the deterministic model and $\lambda = 0.05$ for the stochastic model.



Human	The actual human trajectories observed in the testing set, which are all collision-free.
No action	A policy which outputs an action of zero, maintaining its current speed and direction.
1-step IL	A policy network trained with single-step imitation learning to minimize the negative log-likelihood of the next human action observed in the dataset.
SVG	A policy network trained with stochastic value gradients, using our stochastic forward model. Here the latent variables are inferred using the posterior network for a state trajectory sampled from the training set. This is the same setup as (Heess et al., 2015), with the difference that the agent does not interact with the environment and learns from a fixed observational dataset.
VG	Like SVG, but using the deterministic forward model.
MPIL	-
S-MPIL	-
MPUR	-
S-MPUR	-

(c) Summary of compared methods

Figure 6: Performance on NGSIM dataset.

Figure 5.2 compares performance for the different methods. The 1-step imitation learner, SVG and VG all perform poorly, and do not beat the simple baseline of performing no action. MPUR and MPIL both perform increasingly well with longer rollouts. MPIL performs similarly to the 1-step imitation learner when given a rollout length of 1. This makes sense as they both optimize similar objectives. Training on longer rollouts is essential, as it forces the distribution of states the policy induces and the expert’s distribution to match over longer time horizons.

Videos of the learned policies for both MPIL and MPUR driving in the environment can be found at [url](#). The policy learns effective behaviors such as braking, accelerating and turning to avoid other cars. Figure 7 shows trajectories on the map for different methods. We see that the single-step imitation learner produces divergent trajectories which turn into other lanes, whereas the MPUR and MPIL methods show trajectories which primarily stay on their lanes.

MPUR becomes equivalent to VG in the deterministic setting if we remove the uncertainty penalty, and the large difference in performance shows that including this penalty is essential. Table 8 shows the average predicted policy cost and uncertainty cost of the two methods. VG produces much lower predicted policy cost, yet very high uncertainty cost. This indicates that the actions the policy produces induce a distribution over states which the forward model is highly uncertain about. The policy trained with MPUR produces higher policy cost estimates, but lower uncertainty cost, and performs much better when executed in the environment.

A somewhat surprising finding is that the stochastic model only yields a modest improvement over the deterministic model in the case of stochastic MPUR, despite the improvement in terms of visual

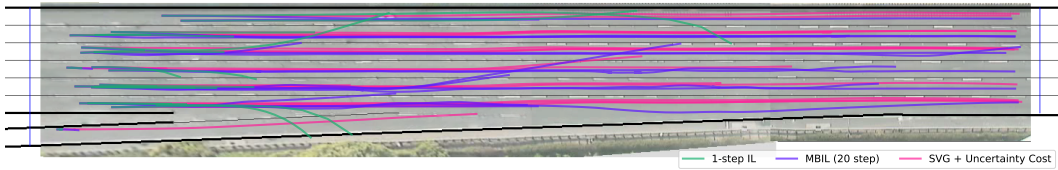


Figure 7: Trajectories

Method	Mean Distance	Success Rate	Total Predicted Cost	U
VG	88.7	0.0	0.03	4087.4
MPUR	976.4	59.1	0.22	1.1

Figure 8: Predictions made by the same forward model for an action sequence produced by a policy trained *with* (top) and *without* (bottom) the epistemic uncertainty cost. Without the uncertainty cost, the policy network learns to output pathological action sequences which produce invalid predictions which nevertheless have low cost.

quality shown in Figure 5, and gives much *worse* performance for MPIL. On further investigation, we found that the forward model becomes less responsive to input actions when it is given latent variables inferred by the posterior network, as opposed to latent variables which are sampled from the prior. This is shown in Appendix E by comparing predictions of the forward model conditioned on different action sequences, using latent variables inferred or sampled from the prior. We also trained a policy network using MPUR with inferred rather than sampled latent variables, and observed a large drop in performance. One possible explanation is that the forward model encodes some factors of variation of the output due to the actions in its latent variables. The sequence of latent variables sampled from the prior are independent, which may cause these effects to cancel each other over the sequence. However, the latent variables inferred from a sequence of states in the training set are highly dependent, and together they may explain away the effects of the actions. This suggests that enforcing independence between actions and latent variables may be necessary to leverage the benefits of stochastic models.

6 CONCLUSION

TODO: improve

In this work we have presented an end-to-end approach for learning driving policies from observational data, which includes preparing a dataset of real-world driving trajectories, adapting it to become a planning environment, training action-conditional forward models, and using them to train policies using with a new uncertainty regularizer which addresses the domain mismatch problem. There are several directions for future work. Although we have applied it here in the context of learning driving policies, the approach is general and could be used in other domains. Furthermore, our current approach does not capture dependencies which are longer than 20 time steps into the future, which corresponds to 2 seconds. We tried two different approaches to capture longer-term dependencies: learning a value function using temporal differences (which in theory can capture arbitrary length dependencies) and unrolling for more time steps, but these did not yield any improvements and sometimes hurt performance. This requires more investigation. Second, it would be interesting to optimize actions or policies to produce more complex and useful behaviors, such as changing to a specified lane while avoiding other cars. In the current setup, the policies are optimized only to avoid collisions and stay within lanes when possible, whereas in a real-world scenario we would want a policy which can safely navigate among traffic to different locations.

ACKNOWLEDGMENTS

Use unnumbered third level headings for the acknowledgments. All acknowledgments, including those to funding agencies, go at the end of the paper.

REFERENCES

- Pulkit Agrawal, Ashvin Nair, Pieter Abbeel, Jitendra Malik, and Sergey Levine. Learning to poke by poking: Experiential learning of intuitive physics. *CoRR*, abs/1606.07419, 2016. URL <http://arxiv.org/abs/1606.07419>.
- C. G. Atkeson and J. C. Santamaria. A comparison of direct and model-based reinforcement learning. In *Proceedings of International Conference on Robotics and Automation*, volume 4, pp. 3557–3564 vol.4, April 1997. doi: 10.1109/ROBOT.1997.606886.
- Mohammad Babaeizadeh, Chelsea Finn, Dumitru Erhan, Roy H. Campbell, and Sergey Levine. Stochastic variational video prediction. *CoRR*, abs/1710.11252, 2017. URL <http://arxiv.org/abs/1710.11252>.
- Nir Baram, Oron Anschel, Itai Caspi, and Shie Mannor. End-to-end differentiable adversarial imitation learning. In *ICML*, 2017.
- Mariusz Bojarski, Davide Del Testa, Daniel Dworakowski, Bernhard Firner, Beat Flepp, Prasoon Goyal, Lawrence D. Jackel, Mathew Monfort, Urs Muller, Jiakai Zhang, Xin Zhang, Jake Zhao, and Karol Zieba. End to end learning for self-driving cars. *CoRR*, abs/1604.07316, 2016.
- Greg Brockman, Vicki Cheung, Ludwig Pettersson, Jonas Schneider, John Schulman, Jie Tang, and Wojciech Zaremba. Openai gym, 2016.
- Kurtland Chua, Roberto Calandra, Rowan McAllister, and Sergey Levine. Deep reinforcement learning in a handful of trials using probabilistic dynamics models. *CoRR*, abs/1805.12114, 2018. URL <http://arxiv.org/abs/1805.12114>.
- Marc Peter Deisenroth and Carl Edward Rasmussen. Pilco: A model-based and data-efficient approach to policy search. In *In Proceedings of the International Conference on Machine Learning*, 2011.
- Emily Denton and Rob Fergus. Stochastic video generation with a learned prior. *CoRR*, abs/1802.07687, 2018. URL <http://arxiv.org/abs/1802.07687>.
- P. Englert, A. Paraschos, J. Peters, and M. P. Deisenroth. Model-based imitation learning by probabilistic trajectory matching. In *2013 IEEE International Conference on Robotics and Automation*, pp. 1922–1927, May 2013. doi: 10.1109/ICRA.2013.6630832.
- Chelsea Finn, Ian J. Goodfellow, and Sergey Levine. Unsupervised learning for physical interaction through video prediction. *CoRR*, abs/1605.07157, 2016. URL <http://arxiv.org/abs/1605.07157>.
- Yarin Gal and Zoubin Ghahramani. Dropout as a bayesian approximation: Representing model uncertainty in deep learning. In Maria Florina Balcan and Kilian Q. Weinberger (eds.), *Proceedings of The 33rd International Conference on Machine Learning*, volume 48 of *Proceedings of Machine Learning Research*, pp. 1050–1059, New York, New York, USA, 20–22 Jun 2016. PMLR. URL <http://proceedings.mlr.press/v48/gall16.html>.
- John Halkias and James Colyar. NGSIM interstate 80 freeway dataset. *US Federal Highway Administration, FHWA-HRT-06-137, Washington, DC, USA*, 2006.
- Nicolas Heess, Gregory Wayne, David Silver, Tim Lillicrap, Tom Erez, and Yuval Tassa. Learning continuous control policies by stochastic value gradients. In C. Cortes, N. D. Lawrence, D. D. Lee, M. Sugiyama, and R. Garnett (eds.), *Advances in Neural Information Processing Systems* 28, pp. 2944–2952. Curran Associates, Inc., 2015.
- Geoffrey E. Hinton, Nitish Srivastava, Alex Krizhevsky, Ilya Sutskever, and Ruslan Salakhutdinov. Improving neural networks by preventing co-adaptation of feature detectors. *CoRR*, abs/1207.0580, 2012. URL <http://arxiv.org/abs/1207.0580>.
- Michael I. Jordan and David E. Rumelhart. Forward models: Supervised learning with a distal teacher. *Cognitive Science*, 16(3):307 – 354, 1992. ISSN 0364-0213. doi: [http://dx.doi.org/10.1016/0364-0213\(92\)90036-T](http://dx.doi.org/10.1016/0364-0213(92)90036-T). URL <http://www.sciencedirect.com/science/article/pii/036402139290036T>.

- Gregory Kahn, Adam Villaflor, Vitchyr Pong, Pieter Abbeel, and Sergey Levine. Uncertainty-aware reinforcement learning for collision avoidance. 02 2017.
- Diederik P. Kingma and Jimmy Ba. Adam: A method for stochastic optimization. *CoRR*, abs/1412.6980, 2014. URL <http://arxiv.org/abs/1412.6980>.
- Diederik P. Kingma and Max Welling. Auto-encoding variational bayes. *CoRR*, abs/1312.6114, 2013. URL <http://dblp.uni-trier.de/db/journals/corr/corr1312.html#KingmaW13>.
- Yann LeCun, Urs Muller, Jan Ben, Eric Cosatto, and Beat Flepp. Off-road obstacle avoidance through end-to-end learning. In Y. Weiss, B. Schölkopf, and J. C. Platt (eds.), *Advances in Neural Information Processing Systems 18*, pp. 739–746. MIT Press, 2006. URL <http://papers.nips.cc/paper/2847-off-road-obstacle-avoidance-through-end-to-end-learning.pdf>.
- Timothy P. Lillicrap, Jonathan J. Hunt, Alexander Pritzel, Nicolas Heess, Tom Erez, Yuval Tassa, David Silver, and Daan Wierstra. Continuous control with deep reinforcement learning. *CoRR*, abs/1509.02971, 2015.
- Rowan McAllister and Carl E. Rasmussen. Improving pilco with bayesian neural network dynamics models. 2016.
- Volodymyr Mnih, Koray Kavukcuoglu, David Silver, Andrei A. Rusu, Joel Veness, Marc G. Belle-mare, Alex Graves, Martin Riedmiller, Andreas K. Fidjeland, Georg Ostrovski, Stig Petersen, Charles Beattie, Amir Sadik, Ioannis Antonoglou, Helen King, Dharmashan Kumaran, Daan Wierstra, Shane Legg, and Demis Hassabis. Human-level control through deep reinforcement learning. *Nature*, 518(7540):529–533, February 2015. ISSN 0028-0836. doi: 10.1038/nature14236. URL <http://dx.doi.org/10.1038/nature14236>.
- Volodymyr Mnih, Adrià Puigdomènech Badia, Mehdi Mirza, Alex Graves, Timothy P. Lillicrap, Tim Harley, David Silver, and Koray Kavukcuoglu. Asynchronous methods for deep reinforcement learning. *CoRR*, abs/1602.01783, 2016.
- Anusha Nagabandi, Gregory Kahn, Ronald S. Fearing, and Sergey Levine. Neural network dynamics for model-based deep reinforcement learning with model-free fine-tuning. *CoRR*, abs/1708.02596, 2017. URL <http://arxiv.org/abs/1708.02596>.
- Karthik Narasimhan, Tejas D. Kulkarni, and Regina Barzilay. Language understanding for text-based games using deep reinforcement learning. *CoRR*, abs/1506.08941, 2015. URL <http://arxiv.org/abs/1506.08941>.
- Nguyen and Widrow. The truck backer-upper: an example of self-learning in neural networks. In *International 1989 Joint Conference on Neural Networks*, pp. 357–363 vol.2, 1989. doi: 10.1109/IJCNN.1989.118723.
- Derrick Nguyen and Bernard Widrow. Neural networks for control. chapter The Truck Backer-upper: An Example of Self-learning in Neural Networks, pp. 287–299. MIT Press, Cambridge, MA, USA, 1990. ISBN 0-262-13261-3. URL <http://dl.acm.org/citation.cfm?id=104204.104216>.
- Junhyuk Oh, Xiaoxiao Guo, Honglak Lee, Richard L. Lewis, and Satinder P. Singh. Action-conditional video prediction using deep networks in atari games. *CoRR*, abs/1507.08750, 2015. URL <http://arxiv.org/abs/1507.08750>.
- Yunpeng Pan, Ching-An Cheng, Kamil Saigol, Keuntaek Lee, Xinyan Yan, Evangelos Theodorou, and Byron Boots. Agile off-road autonomous driving using end-to-end deep imitation learning. *CoRR*, abs/1709.07174, 2017. URL <http://arxiv.org/abs/1709.07174>.
- Razvan Pascanu, Yujia Li, Oriol Vinyals, Nicolas Heess, Lars Buesing, Sébastien Racanière, David P. Reichert, Theophane Weber, Daan Wierstra, and Peter Battaglia. Learning model-based planning from scratch. *CoRR*, abs/1707.06170, 2017.

- Dean A. Pomerleau. Efficient training of artificial neural networks for autonomous navigation. *Neural Computation*, 3:97, 1991.
- Stéphane Ross and J. Andrew Bagnell. Efficient reductions for imitation learning. In *AISTATS*, 2010.
- Stphane Ross, Geoffrey J. Gordon, and Drew Bagnell. A reduction of imitation learning and structured prediction to no-regret online learning. In Geoffrey J. Gordon, David B. Dunson, and Miroslav Dudk (eds.), *AISTATS*, volume 15 of *JMLR Proceedings*, pp. 627–635. JMLR.org, 2011.
- Dorsa Sadigh, Shankar Sastry, Sanjit A. Seshia, and Anca D. Dragan. Planning for autonomous cars that leverage effects on human actions, 06 2016.
- Jurgen Schmidhuber. An on-line algorithm for dynamic reinforcement learning and planning in reactive environments. In *Proceedings of the International Joint Conference on Neural Networks (IJCNN)*, 1990.
- Aravind Srinivas, Allan Jabri, Pieter Abbeel, Sergey Levine, and Chelsea Finn. Universal planning networks. *CoRR*, abs/1804.00645, 2018. URL <http://arxiv.org/abs/1804.00645>.
- Nitish Srivastava, Geoffrey Hinton, Alex Krizhevsky, Ilya Sutskever, and Ruslan Salakhutdinov. Dropout: A simple way to prevent neural networks from overfitting. *Journal of Machine Learning Research*, 15:1929–1958, 2014. URL <http://jmlr.org/papers/v15/srivastava14a.html>.
- Theophane Weber, Sébastien Racanière, David P. Reichert, Lars Buesing, Arthur Guez, Danilo Jimenez Rezende, Adrià Puigdomènech Badia, Oriol Vinyals, Nicolas Heess, Yujia Li, Razvan Pascanu, Peter Battaglia, David Silver, and Daan Wierstra. Imagination-augmented agents for deep reinforcement learning. *CoRR*, abs/1707.06203, 2017.
- G. Williams, N. Wagener, B. Goldfain, P. Drews, J. M. Rehg, B. Boots, and E. A. Theodorou. Information theoretic mpc for model-based reinforcement learning. In *2017 IEEE International Conference on Robotics and Automation (ICRA)*, pp. 1714–1721, May 2017. doi: 10.1109/ICRA.2017.7989202.
- Wojciech Zaremba, Tomas Mikolov, Armand Joulin, and Rob Fergus. Learning simple algorithms from examples. *CoRR*, abs/1511.07275, 2015. URL <http://arxiv.org/abs/1511.07275>.
- Fangyi Zhang, Jürgen Leitner, Michael Milford, Ben Upcroft, and Peter I. Corke. Towards vision-based deep reinforcement learning for robotic motion control. *CoRR*, abs/1511.03791, 2015. URL <http://arxiv.org/abs/1511.03791>.
- Jiakai Zhang and Kyunghyun Cho. Query-efficient imitation learning for end-to-end autonomous driving. *CoRR*, abs/1605.06450, 2016. URL <http://arxiv.org/abs/1605.06450>.

A DATASET AND PLANNING ENVIRONMENT

To begin with, we describe the details and preparation of the dataset and planning environment which we used, which are summarized in Figure 4. The Next Generation Simulation program’s Interstate 80 (NGSIM I-80) dataset (Halkias & Colyar, 2006) consists of 45 minutes of recordings made of a stretch of highway in the San Francisco Bay Area by cameras mounted on a 30-story building overlooking the highway. The recorded area includes six freeway lanes (including a high-occupancy vehicle lane) and an onramp. The driver behavior is complex and includes sudden accelerations, lane changes and merges which are difficult to predict; as such the dataset has high aleatoric uncertainty. There are three time segments, each of 15 minutes, taken at different times of day which capture the transition between uncongested and congested peak period conditions. After recording, a viewpoint transformation is applied to rectify the perspective, and vehicles are identified and tracked throughout the video; additionally, their size is inferred. This yields a total 5596 car trajectories, represented as sequences of coordinates $\{x_t, y_t\}$. We split these trajectories into training (80%), validation (10%) and testing sets (10%).

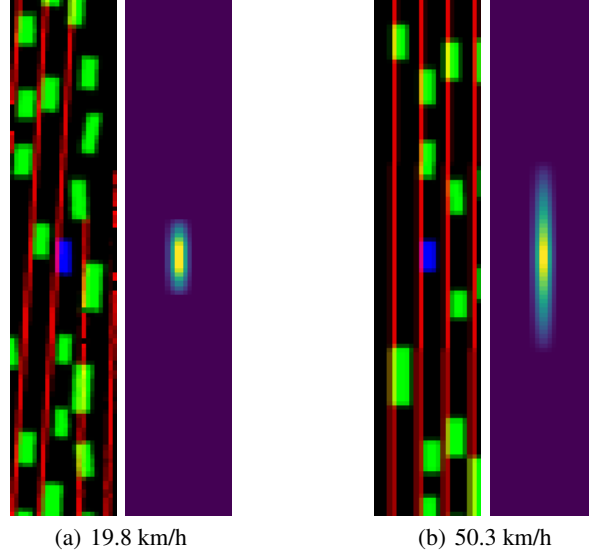


Figure 9: Image state representations and proximity cost masks for cars going at different speeds. The higher the speed, the longer the safety distance required to maintain low cost.

We then applied additional preprocessing to obtain suitable representations for learning a predictive model. Specifically, we extracted the following: i) a state representation for each car at each time step s_t , which encodes the necessary information to choose an action to take, ii) an action a_t which represents the action of the driver, and iii) a cost c_t , which associates a quality measure to each state. We describe each of these below.

State representation: Our state representation consists of two components: an image representing the neighborhood of the car, and a vector representing its current position and velocity. For the images, we rendered images centered around each car which encoded both the lane emplacements and the locations of other cars. Each image has 3 channels: the first (red) encodes the lane markings, the second (green) encodes the locations of neighboring cars, which are represented as rectangles reflecting the dimensions of each car, and the third channel (blue) represents the ego car, also scaled to the correct dimensions. All images have dimensions $3 \times 117 \times 24$, and are denoted by i_t .¹ Two examples are shown in Figure 9. We also computed vectors $u_t = (p_t, \Delta p_t)$, where $p_t = (x_t, y_t)$ is the position at time t and $\Delta p_t = (x_{t+1} - x_t, y_{t+1} - y_t)$ is the velocity.

Action representation: Each action vector a_t consists of two components: an acceleration (which can be positive or negative) which reflects the change in speed, and a change in angle. The acceleration at a given time step is computed by taking the difference between two consecutive speeds, while the change in angle is computed by projecting the change in speed along its orthogonal direction:

$$\begin{aligned}\Delta \text{speed} &= \|\Delta p_{t+1}\|_2 - \|\Delta p_t\|_2 \\ \Delta \text{angle} &= (\Delta p_{t+1} - \Delta p_t)^\top (\Delta p_t)_\perp / \|\Delta p_t\|_2 \\ a_t &= (\Delta \text{speed}, \Delta \text{angle})\end{aligned}$$

¹Another possibility would have been to construct feature vectors directly containing the exact coordinates of neighboring cars, however this presents several difficulties. First, cars can enter and exit the neighborhood, and so the feature vector representing the neighboring cars would either have to be dynamically resized or padded with placeholder values. Second, this representation would not be permutation-invariant, and it is unclear where to place a new car entering the frame. Third, encoding the lane information in vector form would require a parametric representation of the lanes, which is more complicated. Using images representations naturally avoids all of these difficulties.

```

observation = env.reset()
while not done:
    action = policy(observation)
    observation, reward, done, info = env.step(action)
    env.render()

```

Figure 10: NGSIM planning environment.

Cost: Our cost function has two terms: a proximity cost and a lane cost. The proximity cost reflects how close the ego car is to neighboring cars, and is computed using a mask in pixel space whose width is equal to the width of a lane and whose height depends on the speed of the car. Two examples are shown in Figure 9. This mask is pointwise multiplied with the green channel, and the maximum value is taken to produce a scalar cost. The lane cost uses a similar mask fixed to the size of the car, and is similarly multiplied with the red channel, thus measuring the car’s overlap with the lane. Both of these operations are differentiable so that we can backpropagate gradients with respect to these costs through images predicted by a forward model.

This preprocessing yields a set of state-action pairs (s_t, a_t) (with $s_t = (i_t, u_t)$) for each car, which constitute the dataset we used for training our prediction model. We then use the cost function to optimize action sequences at planning time, using different methods which we describe in Section C.

We now describe how we adapted this dataset to be used as an environment to evaluate planning methods. Building an environment for evaluating policies for autonomous driving is not obvious as it suffers from a cold-start problem. Precisely measuring the performance of a given driving policy would require it to be evaluated in an environment where all other cars follow policies which accurately reflect human behavior. This involves reacting appropriately both to other cars in the environment as well as the car being controlled by the policy being evaluated. However, constructing such an environment is not possible as it would require us to already have access to a policy which drives as humans do, which in some sense is our goal in the first place. One could hand-code a driving policy to control the other cars in the environment, however is it not clear how to do so in a way which accurately reflects the diverse and often unpredictable nature of human driving.

We adopt a different approach where we let all other cars in the environment follow their trajectories in the dataset, while controlling one car with the policy we seek to evaluate. The trajectory of the controlled car is updated as a function of the actions output by the policy, while the trajectories of the other cars remain fixed. If the controlled car collides with another car, this is recorded and the episode ends. This approach has the advantage that all other cars in the environment maintain behavior which is close to human-like. The one difference with true human behavior is that the other cars do not react to the car being controlled or try to avoid it, which may cause crashes which would not occur in real life. The driving task is thus possibly made more challenging than in a true environment, which we believe is preferable to using a hand-coded policy. The interface is set up the same way as environments in OpenAI Gym (Brockman et al., 2016), and can be accessed with a few lines of Python code, as shown in Figure 10.

B MODEL DETAILS

The architecture of our forward model consists of four neural networks: a state encoder f_{enc} , an action encoder f_{act} , a decoder f_{dec} , and the posterior network f_{ϕ} . At every time step, the state encoder takes as input the concatenation of 20 previous states, each of which consists of a context image i_t and a 4-dimensional vector u_t encoding the car’s position and velocity. The images i_{t-20}, \dots, i_t are run through a 3-layer convolutional network with 64-128-256 feature maps, and the vectors u_{t-20}, \dots, u_t are run through a 2-layer fully connected network with 256 hidden units, whose final layers contain the same number of hidden units as the number of elements in the output of the convolutional network (we will call this number n_H). The posterior network takes the same input as the encoder network, as well as the ground truth state s_{t+1} , and maps them to a distribution over latent variables, from which one sample z_t is drawn. This is then passed through an expansion layer

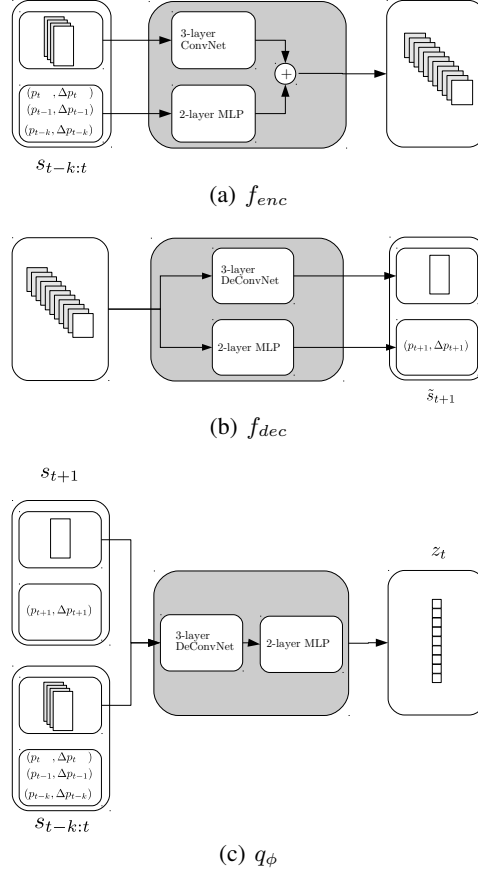


Figure 11: Individual components of the prediction model.

which maps it to a representation of size n_H . The action encoder, which is a 2-layer fully-connected network, takes as input a 2-dimensional action a_t encoding the car’s acceleration and change in steering angle, and also maps it to a representation of size n_H . The representations of the input states, latent variable, and action, which are all now the same size, are combined via addition. The result is then run through a deconvolutional network with 256-128-64 feature maps, which produces a prediction for the next image i_{t+1} , and a 2-layer fully-connected network (with 256 hidden units) which produces a prediction for the next state vector u_{t+1} . These are illustrated in Figure B.

The specific updates of the stochastic forward model are given by:

$$(\mu_\phi, \sigma_\phi) = q_\phi(s_{1:t}, s_{t+1}) \quad (3)$$

$$\epsilon \sim \mathcal{N}(0, I) \quad (4)$$

$$z_t = \mu_\phi + \sigma_\phi \cdot \epsilon \quad (5)$$

$$\hat{s}_{t+1} = (\tilde{i}_{t+1}, \tilde{u}_{t+1}) = f_\theta(s_{1:t}, a_t, z_t) \quad (6)$$

The per-sample loss is given by:

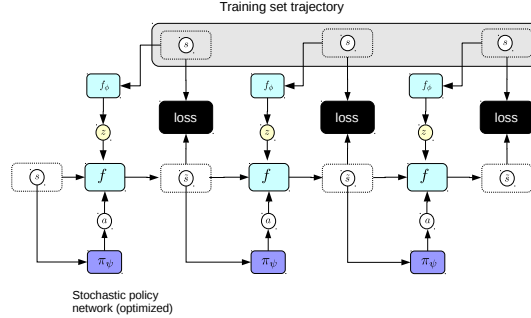
$$\ell(s_{1:t}, s_{t+1}) = \|\tilde{i}_t - i_t\|_2^2 + \|\tilde{u}_t - u_t\|_2^2 + \beta D_{KL}(\mathcal{N}(\mu_\phi, \sigma_\phi) \| p(z)) \quad (7)$$

C PLANNING APPROACHES

We now describe different planning approaches using our stochastic forward model, with diagrams shown in Figure C. It consists of an encoder with an identical architecture as f_{enc} used in the for-

ward model (which also takes 20 consecutive states as input), followed by a 3-layer fully connected network which outputs a 2-D mean and variance (μ, σ) of a diagonal Gaussian over actions.

Two of the planning methods optimize a cost function C , which is a combination of the proximity and lane costs we described previously, as well as an epistemic uncertainty cost which we describe in the next section. For now, we can treat the cost as a scalar-valued differentiable function of a predicted state.



(a) Stochastic Model-Based Imitation Learning (SMBIL)

Figure 12: Planning Methods. SMBIL minimizes the distance between training set trajectories and trajectories predicted by the forward model under the current policy network, using latent variables inferred from the training trajectory. The other methods optimize actions or a policy network to minimize the cost predicted by the forward model, using randomly sampled sequences of latent variables.

C.1 SINGLE-STEP IMITATION LEARNING

The simplest approach to learning a policy from observational data is imitation learning (Pomerleau, 1991), where a network is trained to predict expert actions from states. Here, we give the network a concatenation of 20 states $s_{1:t}$ as input and train it to minimize the negative log-likelihood of the true action observed in the dataset under the parameters of the distribution output by the model:

$$\operatorname{argmin}_{\psi} \left[-\log \mathcal{N}(a_{t+1} | \mu, \sigma) \right], \text{ such that: } (\mu, \sigma) = \pi_{\psi}(s_{1:t})$$

C.2 STOCHASTIC MODEL-BASED IMITATION LEARNING (SMBIL)

We also experimented with a variant of imitation learning using the learned stochastic model, which we found performed better than the standard version. One issue with imitation learning is that errors can accumulate quickly, leading to divergence from the states seen during training. One cause may be that the model is simply minimizing the ℓ_2 loss in action space, which may not correspond to minimizing distances in trajectory space. Consider the following example where an agent is walking exactly along the side of a cliff, and must output an action which represents its angle. To the left is a drop, and to the right is solid ground. Say the expert action is to go straight, i.e. $a_{t+1} = 0$. Now consider two possible actions predicted by the network, $\hat{a}_{t+1} = -\epsilon$ (slight left) and $\hat{a}_{t+1} = +\epsilon$ (slight right). Both of these actions incur the same ℓ_2 cost of ϵ , but have very different consequences. If the agent moves slightly away from the expert action on the left side, they fall off the cliff, which causes a large deviation of their subsequent states from the expert states. If they move slightly to the right however, they stay on solid ground and their subsequent states remain close to the expert states.

As an alternative, we experimented with training a policy to match expert *trajectories*, rather than actions. We do this by unrolling the forward model for multiple timesteps, outputting actions by the policy network using the model predictions, and minimizing the error between the final trajectory

output by the forward model and the expert trajectory observed in the dataset. The motivation here is that if the policy network outputs an action which causes small divergence from the target trajectory at the next timestep, but large divergences later on, it will receive gradients from these larger errors backpropagated through the unrolled forward model.

$$\operatorname{argmin}_{\psi} \left[\sum_{i=1}^T \ell(s_{t+i}, \hat{s}_{t+i}) \right], \text{ such that: } \begin{cases} \hat{s}_t = s_t \\ z_{t+i} = f_{\phi}(\hat{s}_{t+i-1}, \hat{s}_{t+i}) \\ \hat{a}_{t+i} = \pi_{\psi}(\hat{s}_{t+i-1}) \\ \hat{s}_{t+i} = f(\hat{s}_{t+i-1}, \hat{a}_{t+i}, z_{t+i}) \end{cases}$$

C.3 STOCHASTIC VALUE GRADIENTS (SVG)

The last approach which we explored was designed to train a policy network using the learned stochastic forward model, using the framework of Stochastic Value Gradients (Heess et al., 2015). We first randomly sample an initial input state s_t from the training set, sample a sequence of latent variables z to represent a future scenario, and then optimize a parameterized policy network π_{ψ} to minimize the cost predicted by the forward model conditioned on this sequence of latent variables.

$$\operatorname{argmin}_{\psi} \left[\sum_{i=1}^T C(s_{t+i}) \right], \text{ such that: } \begin{cases} z_{t+i} \sim p(z) \\ \hat{a}_{t+i} = \pi_{\psi}(s_{t+i-1}) \\ \hat{s}_{t+i} = f(\hat{s}_{t+i-1}, \hat{a}_{t+i}, z_{t+i}) \end{cases}$$

Our approach differs somewhat from the setup of (Heess et al., 2015), who used latent variables inferred from ground truth trajectories as a means to compensate for model errors. We did not find this to be a problem, possibly because we trained the forward model to make 20-step predictions, whereas they trained the forward model to make single-step predictions.

D TRAINING DETAILS

D.1 FORWARD MODEL

We trained our prediction model in deterministic mode ($p = 0$) for 200,000 updates, followed by another 200,000 updates in stochastic mode. We save the model after training in deterministic mode and treat it as a deterministic baseline. Our model was trained using Adam (Kingma & Ba, 2014) with learning rate 0.0001 and minibatches of size 64, unrolled for 20 time steps, and with dropout ($p_{dropout} = 0.1$) at every layer, which was necessary for computing the epistemic uncertainty cost when training the policy network.

D.2 POLICY MODELS

All policy networks have the same architecture: a 3-layer ConvNet with feature maps of size 64-128-256, followed by 3 fully-connected layers with 256 hidden units each, with the last layer outputting the parameters of a 2D Gaussian distribution over actions. All policy networks are trained with Adam with learning rate 0.0001. The SMBIL and SVG policies are trained by backpropagation through the unrolled forward model using the reparameterization trick (Kingma & Welling, 2013). The single-step imitation learner is trained to directly minimize the negative log-likelihood of the ground truth action in the dataset under the parameters output by the policy network. Both SMPC and SVG models unroll the forward model for 20 steps, and we report results for different unrolling lengths for SMBIL policies.

E ACTION SENSITIVITY